Int. J. Nanosci. Nanotechnol., Vol. 13, No. 4, Dec. 2017, pp. 335-345

Short Communication

Arsenic Removal from Water Samples Using CeO2/Fe2O3 Nanocomposite

Reza Ansari[1,*], Marziyeh Hasanzadeh[1] and Fariba Ostovar[1, 2]

[1]Department of Chemistry, Faculty of science, University of Guilan, Rasht, Iran.
[2]Department of Analytical Chemistry, Environmental research institute, Academic Center Culture & Research, Environmental Engineering, Rasht, Iran.

(*) Corresponding author: ransari271@guilan.ac.ir
(Received: 07 May 2015 and Accepted: 03 August 2016)

Abstract

In the present study, CeO_2/Fe2O3 nanocomposite was prepared by co-precipitation method and its application was investigated for arsenic removal from water. Characterization of the nano sized adsorbent particles was carried out using SEM and XRD techniques. Systemic adsorption experiments were performed in batch systems and the optimum conditions were obtained. The effects of pH, contact time, adsorbent mass, temperature, ionic strength and initial concentration of arsenic were investigated on kinetics and equilibrium of the adsorption. Thermodynamic parameters and adsorption kinetics were studied in detailed to know the nature and mechanism of adsorption. Kinetic studies showed that the adsorption process followed pseudo second order kinetic model. The thermodynamic parameters such as ΔG^0, ΔS^0 and ΔH^0 were calculated, and it was found that the reaction was spontaneous and exothermic in nature. Adsorption equilibrium was studied using Langmuir and Freundlich isotherm models. It was observed that the investigated adsorption process followed Freundlich isotherm. Adsorption capacity (q0) calculated from Langmuir isotherm was found to be 8.260 mg.g-1.The results showed that CeO_2/Fe2O3 nanocomposite particles can be effectively used for the removal of As(III) ions from aqueous solutions.

Keywords: *Adsorption, Arsenic(III) removal, Cerium(IV) oxide, Iron(III) oxide, Nanocomposite.*

1. INRODUCTION

Arsenic is one of the most toxic elements found in groundwater of many regions around the world, especially in Southern and Southeastern Asia [1]. Elevated arsenic concentration in aquatic environments is caused by natural processes such as dissolution of arsenic-containing minerals by weathering, and human activities such as use of arsenical pesticides. There are still over 150 million people around the globe at a risk of regular arsenic uptake through drinking water [2]. To mitigate this situation, the World Health Organization (WHO) has adjusted the maximum permissible limit of arsenic in drinking water from 50 to 10 ppb [3, 4]. There are many treatment technologies for arsenic in subsurface or surface environments. Among them, adsorption technology has been widely used because of its advantages such as easier setup, easier regeneration or disposal of adsorbents, and higher removal efficiency. [5]. Also Several methods of As removal are already available including precipitation, adsorption, ion exchange, solvent extraction, nanofiltration, foam flotation, and biological sequestration [6]. However, as recently noted these technologies cannot perform well in actual field trials, and improved materials and systems are needed [7]. Recently, metal oxide/hydroxides nanomaterials have been exploited extensively for removing arsenic

from contaminated water in view of their rich valence states, variable electronic structures, natural abundance and stability in water solutions, such as iron, zirconium, titanium, manganese and aluminum [7, 8]. Nanoparticles can also be surface modified for environmental applications. Iron nanoparticles have shown improved reactivity by coupling with catalytic metals [9]. In the past few years, it is found that the incorporation of ceria or zirconia into the adsorbents can significantly improve adsorption capacity toward arsenic because they have a unique selectivity for polyoxoanions [10]. Zirconia and ceria in aqueous solutions can form tetra nuclear or octa nuclear species, which have abundant hydroxyl groups and water molecules to be involved in ligand substitution with arsenic species [11]. Thus, composites combined CeO_2 and ZrO_2 might be an ideal candidate material for removing arsenic. Optimizations of CeO_2–ZrO_2 composites, in terms of pore structure, morphology and size, would improve arsenic uptake and kinetics. The greatest threat to public health from arsenic originates from contaminated groundwater. Inorganic arsenic is naturally present at high levels in the groundwater of a number of countries. Drinking water, crops irrigated with contaminated water and food prepared with contaminated water are the sources of exposure. This fact has prompted the need to develop simple, rapid and low-cost techniques for lowering arsenic concentrations in supplied water. In this work, the CeO_2/Fe_2O_3 nanocomposite used as an alternative adsorbent for removing the As(III) ions from aqueous medium.

2. EXPERIMENTAL

2.1. Chemicals

All chemicals used were of analytical grade (AR) and were prepared in distilled water. The sulfate or chloride salts of all cations were purchased from Merck with highest purity available and used without any further purification. 100 ppm of As (III) ion solution prepared by dissolving As_2O_3 in NaOH, and then the pH was brought to 5 using 0.1 M HCl. All experiments were carried out in aqueous solutions using distilled water.

A Metrohm pH meter (Model 827) (Metrohm, Filderstadt, Germany, http://www.metrohmusa.com) with a combined double junction glass electrode, calibrated against two standard buffer solutions at pH 4.0 and 7.0, was used for pH measurement. The pH of the solutions was adjusted using 0.10 M HCl and NaOH solutions.

2.2. Synthesis of CeO_2/Fe_2O_3 Nanostructures

High purity $Ce(SO_4)_2.6H_2O$, $FeCl_3.6H_2O$ and sodium hydroxide were used for preparation of CeO_2/Fe_2O_3 nanocomposite. Initially, 0.10 M of $Ce(SO_4)_2$ and 0.133 M of $FeCl_3$ were prepared. Then, 100 mL of NaOH 0.4 M was added drop wise into 100 mL of well stirring Ce(IV) and Fe(III) mixed solution (equal volume each). The resulting product was stirred for another 2 hr at 100 ^oC under vigorous stirring (500 rpm) and then left for 24 h at room temperature too cool. Then, it was filtered and washed with enough distilled water and left to dry at room temperature. Finally, it was calcined in an air flux by increasing the temperature from room temperature to 500 ^oC with heating rate of 2 ^oC min^{-1}, and holding for 2.5 hr at 500^oC.

2.3. Characterizations

The crystalline structure of the products was characterized by power X-ray diffraction (XRD) using an X'pert PRO X-ray diffractometer at a voltage of 40 kV and a current of 100 mA with Cu K$\propto$ radiation (λ=1.54056 A$^\circ$), in the 2θ ranging from 0 to 70. The surface morphology of fabricated electrode was examined using Scanning electron microscopy (SEM) with unique thermo-emission electron source by a tungsten film, Germany and UK co-production model LEO 1430VP).

2.4. Adsorption study

As_2O_3 was used as the source of As(III). Fixed amounts of dry CeO_2/Fe_2O_3 (50 mg) were directly added into beakers containing 25 mL of 10 mg L^{-1} As(III) solutions with different pH for 1 h. During this process, the beaker was shaken in a thermostatic shaker bath, operating at 25 ^oC and 100 rpm. The pH of the As(III) solution was adjusted by either 0.1 M HCl or 0.1 M NaOH solutions. The analysis of As(III) was carried out using coulometric titration [12,13]. In coulometric titration, the end point was detected with high precision employing potentiometrically employing Pt and Ag/AgCl in KCl 3M as indicator and reference electrodes respectively. All As(III) solutions were used at neutral pH and performed at room temperature. The removal percentage of As(III) removal (R) can be calculated by the following equation:

$$\% R = (C_0 - C_e/C_0) \times 100 \quad (1)$$

where C_0 is the initial concentration of As(III) in solution (mg L^{-1}) and C_e is the equilibrium concentration (mg L^{-1}). The adsorption isotherms for As(III) were established by batch adsorption experiments. 50 mg CeO_2/Fe_2O_3 was immersed into 25 mL As(III) solutions with different concentration. The initial pH of the As(III) solutions was adjusted to 5.0 by using 0.1 M HCl. The adsorption was carried out at 25 ˚C with constant shaking, and then kept for 1 h to establish adsorption equilibrium. The equilibrium adsorption capacity was determined using the following equation:

$$q_e = (C_0 - C_e)V/W \quad (2)$$

where C_o is the initial concentration of As(III) in solution (mg L^{-1}), C_e is the equilibrium concentration (mg L^{-1}), q_e is the equilibrium adsorption capacity (mg L^{-1}), m is the mass of adsorbent (g), and V is the volume of solution (L). The kinetic adsorption performance was studied by contacting 100 mg of CeO_2/Fe_2O_3 with As(III) solutions of different initial concentration at 25 ^oC. The initial pH of the As(III) solution is 5.0, and the solution was shaken during the process. The adsorption capacity was calculated by the following equation:

$$q_t = (C_0-C_t)V/W \quad (3)$$

where q_t is the adsorption capacity at time t, C_o is the initial concentration of As(III) in solution (mg L^{-1}), C_t is the As(III) concentration at time t (mg L^{-1}), m is the mass of adsorbent (g), and V is the volume of solution (L).

2.5. Application in Real Samples

The drinking water and a pond water sample were also used as real samples to access the arsenic removal efficiency of the developed adsorbent. These were then spiked with 10 mg/L of As(III) and adjusted to pH 5 and 50 mg of the adsorbent was added into each spiked sample and stirred for 60 min at room temperature then the remaining arsenic concentration was determined by coulometric titration.

3. RESULTS AND DISCUSSION

3.1. XRD Studies

Figure 1 shows XRD patterns of Fe_2O_3 NPs, CeO_2 NPs and Fe_2O_3–CeO_2 composites. The pure CeO_2 reflections observed at 2θ= 28.60° (111), 33.20° (200), 47.40° (220), 56.40°(311), 59.10° (222) and 69.40° (400) are related to fluorite structure (cubic) according to the Joint Committee Powder Diffraction Standards (JCPDS) file no. 081-0792 [14]. The pure Fe_2O_3 displays a typical XRD pattern of hematite, a-Fe_2O_3 (hexagonal) and the positions and relative intensities of all peaks agreed well with those derived from the standard JCPDS patterns (patterns for standard hematite (JCPDS #33-0664, a ¼ 5.035^{0}A)). These results supported that the resultant material had a pure-phase hematite crystal structure. Hematite (a-Fe_2O_3), have been detected. The diffraction

peaks corresponding to the (1 0 4), (1 1 0), (1 1 3), (0 2 4), (1 1 6), (0 1 8), (2 1 4), and (3 0 0) planes provided clear evidence for a pure hexagonal structure [15]. It can be seen that, Diffraction patterns of CeO_2/Fe_2O_3 nanocomposites showed the combination of XRD profiles of both CeO_2 and Fe_2O_3 nanoparticles structures. The formation of Fe–Ce oxide solid solution has been reported to depend on the preparation method, particularly on the final calcinations temperature. studied the effect of calcinations temperature on the structure of Fe50-Ce50 mixed oxides prepared by co-precipitation, in which Fe 50 % -Ce 50% formed a solid solution upon calcinations at 573 K whereas Fe segregated from the solid solution and formed hematite when the calcinations temperature increased to 773 K and 973 K [16]. Fe 50 % -Ce 50% structure means the equal grams to any of nanoparticles in the nanocomposite. As shown in Figure 1, when the percentage composition is about 50% -50%, four peaks seen in the region of 29º, 33º, 48º and 57º were respectively indexed as (111), (110), (024), (311) planes for fluorite and hematite of CeO_2 and Fe_2O_3 NPs structures that the results agrees well with previous results [17].

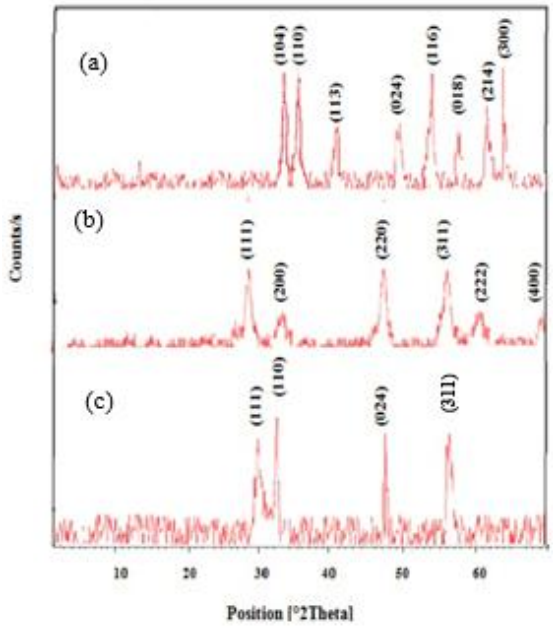

Figure 1. *XRD patterns of (a) Fe_2O_3 NPs, (b) CeO_2 NPs and (c) Fe_2O_3–CeO_2 composites.*

3.2. SEM Studies

Scanning electron microscope (SEM) pictures are useful for examining the fine structure of materials. SEM technique is commonly used for surface characterization and determination of particle size, shape as well as particle size distribution in nanomaterials. The scanning electron microscope (SEM) micrographs of the synthesized pure CeO_2 and CeO_2/Fe_2O_3 composite are shown in (Figures 2).

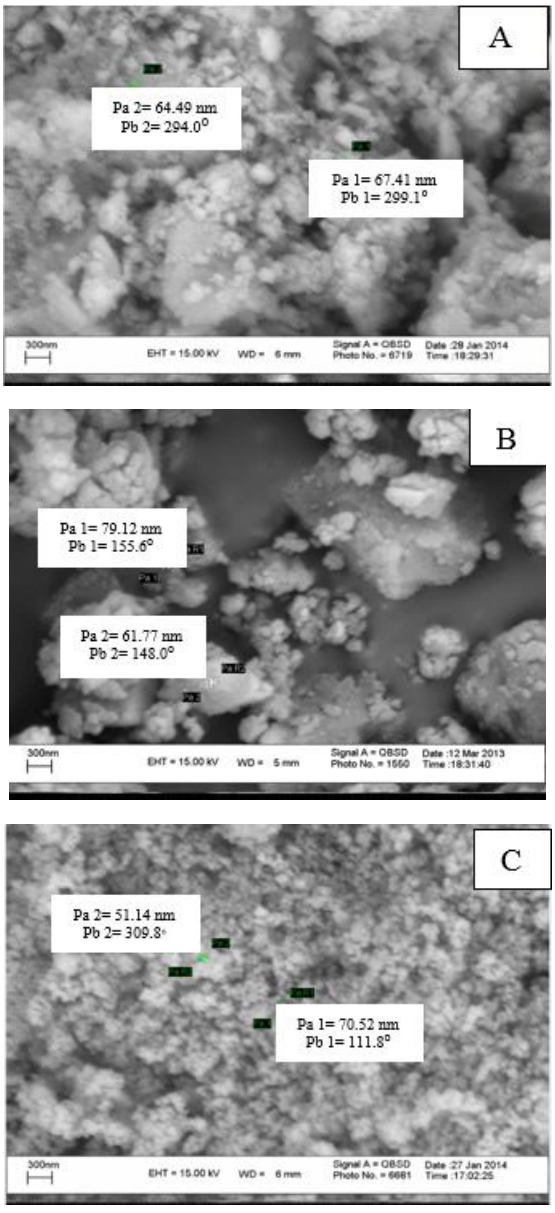

Figigure 2. *SEM images of: (A) CeO_2 NPs, (B) Fe_2O_3 NPs and (C) CeO_2 / Fe_2O_3 NC*

3.3. Effect of pH

To investigate the effect of pH, As(III) solution (25 mL, C=10 mg L^{-1}) was treated with 50.0 mg portions of dried sorbent (CeO_2, Fe_2O_3 and CeO_2/Fe_2O_3) at various pH (2–10). The results obtained are depicted in (Figure 3). It is found that the adsorption capacity is highly dependent on the pH of the solution. The maximum adsorption capacities at different initial concentration solutions were all achieved at pH 5-6, in which As(III) exist mostly natural H_3AsO_3 form. At more alkaline pH, anionic As(III) species ($H_2AsO_3^-$ and $HAsO_3^{2-}$) predominate and the surface of the adsorbent is also negatively charged, thus making more difficult the interaction between arsenic and the adsorbent.

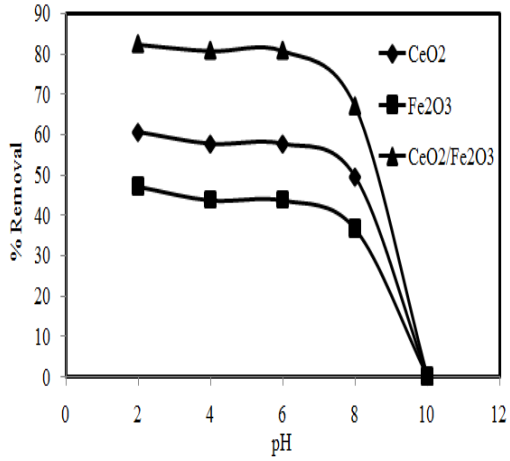

Figure 3. *The effect of initial solution pH on the adsorption of As (III) ions. (T = 25 ºC, t= 60 min, C_0= 10 ppm and m= 50.0 mg).*

3.4. Effect of Contact Time

The saturation time of adsorbents was obtained by plotting the removal efficiency of As(III) against time (Figure 4). As(III) solution (25 mL, C=10 mg L^{-1}) was treated with 50 mg of selected adsorbent (CeO_2, Fe_2O_3 and CeO_2/Fe_2O_3) for different periods of time (10–120 min) with stirring at room temperature. The results indicate higher removal efficiency observed for CeO_2/ Fe_2O_3 at all exposure times compared to CeO_2 and Fe_2O_3 adsorbents. Removal of As(III) using CeO_2/Fe_2O_3 is also very favorable from the kinetic point of view. Removal of As(III) higher than 60% occurred at the initial stage of exposure (within 20 min).

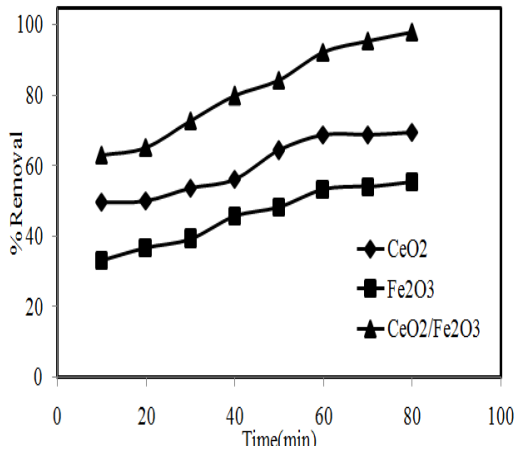

Figure 4. *The effect of contact time on the adsorption of As (III) ions. (T = 25 ºC, pH= 5.0, initial concentration= 10 mg/L and dose of adsorbent= 50.0 mg).*

3.5. Effect of Adsorbent Mass

The dosage of adsorbent used in the adsorption process is an important factor, which determines the capacity of adsorbent for a given initial concentration of heavy metal ion solution. To study the dosage effect on the As(III) removal performance, different amount of CeO_2, Fe_2O_3 and CeO_2/Fe_2O_3 were added into 10 ppm As(III) solution (pH 5.0) for 1 h. The results are shown in (Figure 5). The results indicated that the percentage removal of As(III) rapidly increased with the increase of dosage. The increase of percentage removal of As(III) due to the more available sorption sites.

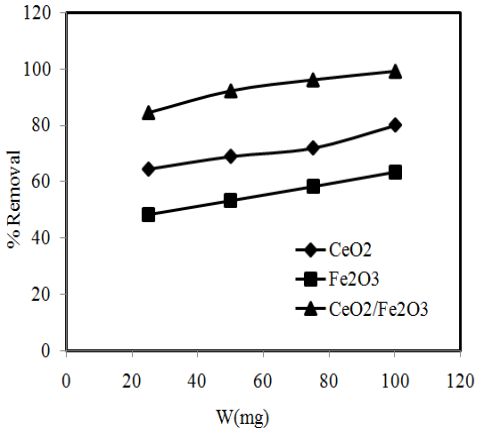

Figure 5*. The effect of adsorbent mass on the As(III) ions removal. (T = 25 ºC, pH= 5.0, t = 60 min and C_i= 10 mg/L).*

3.6. Effect of Initial Concentration

To study the effect of initial concentration of As(III) on its adsorption, As(III) solution (25 mL, C_0=5-100 mg L^{-1}) was treated with 0.50 g of different adsorbents (CeO_2, Fe_2O_3 and CeO_2/Fe_2O_3) at optimum pH value with moderate shaking and at room temperature for 1 h. Triplicate samples were measured for each initial concentration and the data reported are the average of the measurements with high precision. The results obtained are presented in (Figure 6). As our results show, at any concentration of As(III), higher sorption percentage was observed for CeO_2/Fe_2O_3 compared to other adsorbents.

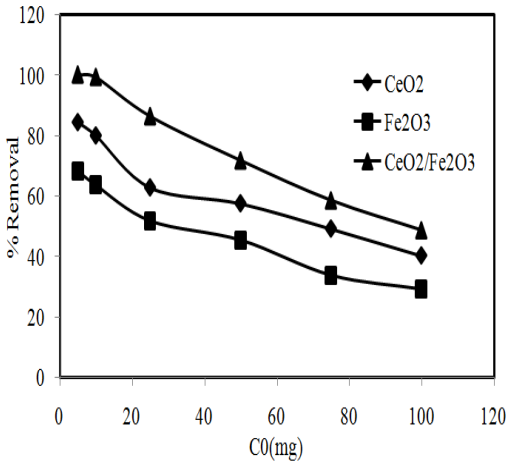

Figure 6. *The effect of initial concentration of As(III) ions onto the adsorbent* **(***T = 25 ◦C, pH= 5.0, t = 60 min and dosage of adsorbent= 50.0 mg)*

3.7. Effect of Ionic Strength

The effect of ionic strength on the adsorption of As(III) onto the CeO_2/Fe_2O_3 was studied by carrying out a series of experiments at varying concentrations of NaCl and $CaCl_2$ solutions. The pH of the As(III) solution was adjusted to 5.0 before adsorption. The results showed that the adsorption capacity didn't change with the increase of ionic strength.

3.8. Adsorption Kinetics

In order to investigate the mechanism of process and potential rate controlling steps such as mass transfer and chemical reaction, the experimental kinetic data for the uptake of As(III) ions were modeled by the pseudo-first-order and the pseudo-second-order equations [18], given in (Equations 4 and 5), respectively:

$$log(q_e - q_t) = log(q_e) - \frac{K_1}{2.303} t \qquad (4)$$

$$\frac{t}{q_t} = \frac{1}{K_2 q_e^2} + \frac{1}{q_e} t \qquad (5)$$

The correlation coefficients for the first order kinetic model were determined and compared with that of second order kinetic model. It is seen that the correlation coefficient of first order kinetic are lower than in the case of second order kinetic model (Table 1). This shows that kinetics of As(III) ions adsorption by CeO_2/Fe_2O_3 are better described by pseudo-second order kinetic model rather than pseudo first order model. The linearity of the plot (figure not shown) also shows the applicability of the pseudo-second order kinetic model, which has average regression coefficient of R^2=0.997. Also, $q_{e(cal)}$ using pseudo-second order kinetic model is approximately equal to $q_{e(exp)}$, which has been obtained experimentally.

3.9. Thermodynamic Studies

Thermodynamic considerations of an adsorption process are necessary to conclude whether the process is spontaneous or not [19]. The Gibbs free energy change, ΔG°, is an indication of the spontaneity of a chemical reaction. At a given temperature, if ΔG° is a negative value, Reactions occur spontaneously. Thermodynamic constants of Gibb's free energy change, ΔG°, enthalpy change, ΔH°, and entropy change, ΔS°, are

Table 1. *Rate constants obtained from kinetic studies.*

C_0 ($mg\ .L^{-1}$)		10	25	50
$q_{e(exp)}$ ($mg\ g^{-1}$)		2.21	5.39	8.96
Pseudo-First Order rate constants	K_1 (min^{-1})	0.0321	0.0368	0.044
	$q_{e(cal)}$ ($mg\ g^{-1}$)	1.202	1.140	1.729
	R^2	0.946	0.936	0.878
Pseudo-Second Order rate constants	K_2 ($g.\ mg^{-1}\ min^{-1}$)	0.041	0.089	0.610
	$q_{e(cal)}$ ($mg.\ g^{-1}$)	2.51	5.43	9.09
	R^2	0.995	0.962	0.938

calculated using the following relations:

$$\Delta G^{\circ} = -RT\ \ln K_a \qquad (6)$$

$$\Delta G^{\circ} = \Delta H^{\circ} - T\Delta S^{\circ} \qquad (7)$$

where K_d is the distribution coefficient for the adsorption, T is the solution temperature (K) and R is the gas constant. ΔH^{o} and ΔS^{o} were calculated from the slope and intercept of Van't Hoff plots of $\ln K_d$ versus 1/T [17]. The results are listed in (Table 2).

The negative values of ΔG° indicate that the adsorption of As(III) ions on adsorbent is spontaneous. It can also be

Table 2. *Thermodynamic parameters obtained from thermodynamic studies.*

C_0 ($mg\ L^{-1}$)	T (K)	10	25	50
ΔH° (kJ/mol)	298	-5.48	-2.64	-0.73
$\Delta S^{\circ} \times 10^4$ (kJ/mol.K)	298	3.02	70	53
- ΔG° (kJ/mol)	278	5.42	4.34	2.10
	298	5.57	4.55	2.31
	308	5.66	4.58	2.33
	328	5.78	4.66	4.77
	338	5.90	4.77	2.51

noted that the change in free energy decreases with increase in temperature, which exhibits an increase in adsorption with the rise in temperature. The negative value of change in enthalpy (ΔH°) shows that the adsorption is an exothermic process, while positive value of change in entropy (ΔS°) reflects the increased randomness at the solid/solution interface.

3.10. Adsorption Isotherms

Adsorption isotherm is basically important to describe how solutes interact with adsorbents, and is critical in optimizing the use of adsorbents. The adsorption isotherms of CeO_2/Fe_2O_3 for As(III) removal are carried out at varied concentrations ranging from 5.0 to 100 mg L^{-1}, and the result is shown in (Table 3). The adsorption isotherms were studied by two common adsorption models: Langmuir and Freundlich isotherm models. A basic assumption of the Langmuir theory is that sorption takes place at specific homogeneous sites within the adsorbent. Compared to the Langmuir isotherm, the Freundlich mode is generally found to be

better suited for characterizing multi-layer adsorption process [20].

The Langmuir isotherm is expressed:

$$\frac{1}{q_e} = \frac{1}{q_m} + \frac{1}{K_L q_m} \times \frac{1}{C_e} \qquad (8)$$

where C_e is the equilibrium concentration of adsorbate (mg L^{-1}), q_e is the amount of metal adsorbed per gram of the adsorbent at equilibrium (mg g^{-1}), q_m is maximum monolayer coverage capacity (mg g^{-1}) and K_L is the Langmuir isotherm constant (L mg^{-1}) [20]. q_{max} and K_L are calculated from the slopes and intercepts of the straight lines of plot of $1/q_e$ versus $1/C_e$. The Freundlich adsorption isotherm can be expressed as:

$$\log \frac{X}{m} = \log K_F + \frac{1}{n} \log C_e \qquad (9)$$

where X/m is the equilibrium adsorption capacity (mg g^{-1}), Ce is the equilibrium or residual concentration (mg L^{-1}) of As(III) in the solution, and K_F and 1/n are empirical Freundlich constants indicating sorption capacity of the adsorbent and intensity of the adsorption (mg g^{-1}), respectively. In the Freundlich adsorption system, values of n and K_F were calculated from the slope and intercept of the linear plot of log X/m against log Ce (Table 3). The Freundlich equation deals with physicochemical adsorption on heterogeneous surfaces. For a good adsorbent, the n value is usually between 1 and 10 which is indicative of surface heterogeneity [21].

The values of q_{max}, K_L, K_F, 1/n and the correlation coefficients for Langmuir and Freundlich are given in (Table 3). It can be seen that the Freundlich model yields a much better fit than the Langmuir model. This, however, is indicative of the heterogeneity of the adsorption sites on the clay particles. From (Table 3), it is noted that the values of n are bigger than 1, indicating that the sorption of As(III) ions onto CeO_2/Fe_2O_3 is favorable. Furthermore, the value of K_F is 5.0 for As(III). Furthermore, from the data calculated in (Table 3), the R_L is greater than 0 but less than 1 indicating that Langmuir isotherm is favorable. From this research work, the maximum monolayer coverage capacity q_m from Langmuir Isotherm model was determined to be 8.260 mg g^{-1}, K_L (Langmuir isotherm constant) is 5.500 L mg^{-1} ,R_L (the separation factor) is 0.018 indicating that the equilibrium sorption was favorable and the R^2 value is 0.871 proving that the sorption data fitted fairly well to Langmuir Isotherm model.

The correlation coefficient values (R^2) obtained shows that the equilibrium data fit better with the Freundlich model as compared to Langmuir model in the concentration range studied. As the R^2 value is slightly higher for the Freundlich isotherm, the adsorption appears to be through physio-sorption and has a heterogeneous surface composed of different classes of adsorption sites [22]. The value of the Freundlich parameter (n=4.4) shows favorable adsorption of As(III) onto CeO_2/Fe_2O_3 . High value of n indicates a strong bond between the adsorbent and the adsorbate. Table 4 compares the optimum result and maximum adsorption capacity from this study with some other research works for removal of arsenic(III) by different hybrid materials, nanoparticles, composites and nanocomposites from solutions.

3.11. Interference study

This experiment was designed to evaluate the interference against arsenic adsorption by common anions including phosphate (PO_4^{3-}), sulphate (SO_4^{2-}) and chloride (Cl^-). Each interfering ion at various concentration of 1, 10 and 50 mg/L was added into 10 mg/L of arsenic solution as binary mixtures. The mixtures were then subject to the arsenic removal using 50 mg of adsorbent at pH 5 for 1 h. The results showed that, the higher concentration of interference ions, especially, PO_4^{3-} and SO_4^{2-}, caused significant decreases of

Table 3. *Adsorption isotherm constants for adsorption of As(III).*

Langmuir	q_m	mg g^{-1}	8.260
	K_L	L mg^{-1}	5.500
	R_L		0.018
	R^2		0.871
Freundlich	K_F	mg g^{-1} $(mg/L)^{-1/n}$	5.000
	n		4.405
	R^2		0.993

Table 4: *Comparison As(III) adsorption capacity (q_m, $mg.g^{-1}$) with some adsorbent materials*

Adsorbents	Adsorption Capacity ($mg.g^{-1}$)	Reference
Fe(II) and Fe(III) loaded loaded apricot, stone-based ACs	2.02	[23]
GFH (granular ferric hydroxide)	8.00	[24]
ZrPACM-43	0.20	[25]
Magnetic hematite-coated Fe_3O_4 particles	1.00	[26]
Fe_3O_4-RGO–MnO_2 nanocomposites	14.04	[27]
Magnetite nanoparticles	3.7	[28]
Ce–Ti oxide adsorbent	6.8	[29]
CeO_2/Fe_2O_3 nanocomposite	8.26	Present study

arsenic removal efficiency probably because these ions have oxyanion structure similar to those of As(III).

3.12. Application in Real Samples

The drinking water samples from different manufacturer and a pond water were also used to evaluate the arsenic removal efficiency of the developed adsorbent. All of these samples originally contain no arsenic and thus were spiked with 10 mg/L As(III). The adsorbent was allowed to adsorb As(III) from these solutions under the optimal conditions and the remaining arsenic concentration was determined .

It was found that the arsenic removal from the drinking water sample exhibited the highest adsorption efficiency of 92 %, while the efficiencies of the pond water were lower because they are mineral water that normally contain relatively high level of potential interfering mineral ions. Hence, the arsenic adsorption by the CeO_2/Fe_2O_3 nanocomposite was best achieved when the samples contain no or masked off interference ions.

4. Conclusion

Application of CeO_2/Fe_2O_3 nano composite can be considered as an efficient adsorbent for As(III) ions removal from aqueous solutions. Based on the adsorption isotherms, the adsorption data fitted well to Freundlich equation. Sorption kinetic data revealed that the adsorption kinetics for CeO_2/Fe_2O_3 NC conform pseudo second order equation. This suggests a chemisorption mechanism during As(III) ions uptake by adsorbent. Negative values of ΔG° indicate the spontaneous nature of adsorption. Negative values obtained for ΔH° and positive values obtained for ΔS° for CeO_2/Fe_2O_3 NC, indicate that sorption process is exothermic and the spontaneity of the reaction is therefore controlled by both enthalpy and entropy factors.

ACKNOWLEDGMENTS

The authors appreciate the Research Department of university of Guilan for partially financial support of this work.

REFERENCES

1. Winkel, L. H., Trang, P. T. K., Lan, V. M., Stengel, C., Amini, M., Ha, N. T., Viet, P. H., Berg, M. (2011). "Arsenic pollution of groundwater in Vietnam exacerbated by deep aquifer exploitation for more than a century", *P. N.A.S*, 108:1246-1251.
2. Kleinert, S., Muehe, E. M., Posth, N. R., Dippon, U., Daus, B., Kappler A. (2011). "Biogenic Fe (III) minerals lower the efficiency of iron-mineral-based commercial filter systems for arsenic removal", *Environ. Sci. Technol*., 45: 7533–7541.
3. Javier, M. A. B., Arcibar-Orozco, A., J. Rangel-Mendez, Rene. (2012). "Effect of Phosphate on the Particle Size of Ferric Oxyhydroxides Anchored onto Activated Carbon: As(V) Removal from Water", *Environ. Sci. Technol*., 46: 9577–9583.
4. McArthur, J. M.m Banerjee, D. M., Hudson-Edwards, K. A., Mishra, R., Purohit, R., Ravenscroft, P., Cronin, A., Howarth, R. J., Chatterjee, A., Talukder, T., Lowry, D., Houghton, S., Chadha D. K. (2004). "Natural organic matter in sedimentary basins and its relation to arsenic in anoxic ground water: the example of West Bengal and its worldwide implications", *Appl. Geochem*., 19: 1255–1293.
5. Gimenez, J., Martinez, M., de Pablo, J., Rovira, M., Duro L. (2007). "Arsenic sorption onto natural hematite, magnetite, and goethite", *J. Hazard. Mater*., 141: 575-580.
6. Mayoa, J. T., Yavuza, C., Yeanb, S., Congb, L., Shipleyb, H., Yua, W., Falknera, J., Kanb, A., Tomsonb, M., Colvina V. L. (2007). "The effect of nanocrystalline magnetite size on arsenic removal", *Sci. Tech. Adv. Mater*., 8: 71-75.
7. Mertens, J., Rose, J., Kagi, R., Chaurand, P., Plotze, M., Wehrli, B., Furrer G. (2012). "Adsorption of arsenic on polyaluminum granulate", *Environ. Sci. Technol*., 46: 7310–7317.
8. Nieto-Delgado, C., Rangel-Mendez J. R. (2012). "Anchorage of iron hydro (oxide) nanoparticles onto activated carbon to remove As (V) from water", *Water Res*. 46: 2973–2982.
9. Obare, S. O., Meyer G. J. (2004). "Nanostructured materials for environmental remediation of organic contaminants in water", *J. Environ. Sci. Health A*, 39: 2549–2582.
10. Biswas, B. K., Inoue, J. I., Inoue, K., Ghimire, K. N., Harada, H., Ohto, K., Kawakita, H. (2008). "Adsorptive removal of As (V) and As (III) from water by a Zr (IV)-loaded orange waste gel", *J. Hazard. Mater*., 154: 1066–1074.
11. Zhang, Y., Dou, X. M., Zhao, B., Yang, M., Takayama, T., Kato, S. (2010). "Removal of arsenic by a granular Fe–Ce oxide adsorbent: fabrication conditions and performance", *Chem. Eng. J*., 162: 164–170.
12. Ansari, R., Alizadeh, N., Shademan, S.M. (2013). "Application of silica gel/polyaniline composite for adsorption of ascorbic acid from aqueous solutions", *Iran. Polym. J*., 22: 739-748.
13. Biswas, S.D., Dey, A.K. (1963). "Coulometric Determination of Arsenic (III) and antimony (III)", *J für Praktische Chemie*., 21:147–148.
14. Chaiwichian, S., Inceesungvorn, B., Pingmuang, K., Wetchakun, K., Phanichphant, S., Wetchakun, N. (2012). "Synthesis and characterization of the novel $BiVO_4/CeO_2$ nanocomposites", *Eng. J*., 16: 153-160.
15. Yu B.Y., Kwak, S. Y. (2012). "Carbon quantum dots embedded with mesoporous hematite nanospheres as efficient visible light-active photocatalysts", *J. Mater. Chem*, 22: 8345-8353.
16. Pe´rez-Alonso, F. J., Lo´pez Granados, M., Ojeda, M., Terreros, P., Rojas, S., Herranz, T., Fierro, J. L. G., Gracia, M., Gancedo, J. R. (2005). "Chemical structures of coprecipitated Fe-Ce mixed oxides", *Chem. Mater*., 17: 2329-2339.
17. Bao, H., Chen, X., Fang, J., Jiang, Z., Huang, W. (2008). "Structure-activity relation of Fe_2O_3–CeO_2 composite catalysts in CO oxidation", *Catal. Lett*., 125: 160–167.
18. Weber, W. J., Morris, J. C. (1963). "Kinetics of adsorption on carbon from solution", *J. Sanit. Eng. Div. Am. Soc. Civ. Eng*., 89: 31–60.
19. Hong, S., Wen, Ch., He, J., Gan, F., Ho Y. Sh. (2009). "Adsorption thermodynamics of Methylene Blue onto bentonite", *J. Hazard. Mater*., 167: 630-633.
20. Langmuir, I. (1918). "The adsorption of gases on plane surfaces of glass, mica and platinum", *J. Am. Chem. Soc*., 40: 1362-1403.
21. Aharoni, C., Ungarish M. (1977). "Kinetics of activated chemisorption. Part 2.—Theoretical models", *J. Chem. Soc. Faraday Trans 1*, 73: 456–464.
22. Mahanta, N., Valiyaveetti, S. (2013). "Functionalized poly(vinyl alcohol) based nanofibers for the removal of arsenic from water", *RSC Adv*., 3: 2776–2783.
23. Tuna, A. Ö. A., Özdemir, E., Şimşek, E. B., Beker, U. (2013). "Removal of As (V) from aqueous solution by activated carbon-based hybrid adsorbents: Impact of experimental conditions", Chemical. Eng. J., 223: 116–128.
24. Badruzzaman, M., Westerhoff, P., Knappe, D.R.U. (2004). "Intraparticle diffusion and adsorption of arsenate onto granular ferric hydroxide (GFH)", *Water Res*., 38(18): 4002–4012.
25. Mandal, S., Sahu, M. K., Patel, R. K. (2013). "Adsorption studies of arsenic (III) removal from water by zirconium polyacrylamide hybrid material (ZrPACM-43)", *Water Res. Industry*., 4: 51–67.

26. Sabbatini, P., Rossi, F., Thern, Marajofsky, G. A., de Cortalezzi, M.M.F. (2009). “Iron oxide adsorbers for arsenic removal: a low cost treatment for rural areas and mobile applications”, *Desalination*., 248: 184–192.
27. Luo, X., Wang, Ch., Luoa, Sh., Dong, R., Tu, X., Zeng, G. (2012). “Adsorption of As (III) and As (V) from water using magnetite Fe_3O_4-reduced graphite oxide–MnO_2 nanocomposites”, *Chem. Eng. J.*, 187: 45– 52.
28. Chowdhury, S.R., Yanful, E.K., (2011). "Arsenic removal from aqueous solutions by adsorption on magnetite nanoparticles", *Water Environ. J.*, 25: 429–437.
29. Zhijian, L., Shubo, D., Guang, Y., Jun, H., Lim, V.C. (2010). “As (V) and As (III) removal from water by a Ce–Ti oxide adsorbent: behavior and mechanism”, *Chem. Eng. J.*, 161: 106–113.